Available online at www.sciencedirect.com
ScienceDirect
Trans. Nonferrous Met. Soc. China 25(2015) 3893−3903
Transactions of Nonferrous Metals Society of China
www.tnmsc.cn

Dry sliding wear characterization of Al 6061/rock dust composite

K. SOORYA PRAKASH[1], A. KANAGARAJ[2], P. M. GOPAL[1]

1. Department of Mechanical Engineering, Anna University Regional Campus, Coimbatore 641046, India;
2. Department of Mechanical Engineering, Akshaya College of Engineering and Technology, Coimbatore 642109, India

Received 24 February 2015; accepted 21 July 2015

Abstract: The influence of rock dust size (10−30 μm) and mass fraction (5%−15%) on density, hardness and dry sliding wear behavior of Al 6061/rock dust composite processed through stir casting was investigated. Wear behavior of the developed composite was characterized at different loads, sliding velocities and distances using pin-on-disc setup. The experiments were conducted based on Taguchi's L27 orthogonal array and the influence of process parameters on wear rate was studied using ANOVA. The experimental results reveal that the applied load and reinforcement size are the major parameters influencing the specific wear rate for all samples, followed by mass fraction of reinforcement, sliding velocity and sliding distance at the level of 47.61%, 28.57%, 19.04%, 9.52% and 4.76%, respectively. The developed regression equation was tested for its accuracy and made evident that it can be used for predicting the wear rate with minimal error. With the help of SEM images, the worn surfaces of the novel composite were studied and the analysis proves that the wear resistance of aluminium alloys can be well improved with the addition of rock dust as reinforcement.

Key words: aluminium metal matrix composite; rock dust; stir casting; wear; ANOVA

1 Introduction

Aluminum metal matrix composites (Al MMCs) are used globally in variety of structural and tribological applications because of their superior properties such as high specific modulus, strength, hardness, low density, excellent wear resistance, low heat expansion coefficient and stable properties at elevated temperatures [1,2]. In recent years, the aerospace applications have propelled the development of high-temperature aluminum alloys for the reason being capable of competing with titanium alloys [3,4]. The increased use of Al MMCs has found its way as a substitute for cast iron in brake rotors/discs used for ground transportation systems including passenger cars and trains [5,6]. Further, studies are in progress to optimize the properties and chemical formulation of both disc and brake pad in order to achieve superior performance during braking.

Aluminium 6061 alloys with good corrosion resistance and workability were employed in valves, brake components and certain other similar applications, but their wear resistance is somewhat lower when compared with conventional hard materials in use. Nevertheless, wear is the main cause for the failure of materials. To widen the applications of these materials, recent researches have been oriented towards improving wear resistance and high specific strength for their ultimate advantages.

MMCs developed by reinforcing fly ash and silicon carbide with aluminium using conventional techniques exhibit increasing trend for many properties with the increase in reinforcement level, except for density which decreases with the increase in reinforcements [7,8]. Researchers concentrate both on experimental and analytical portions of Al MMCs to gain better mechanical properties and excellent wear resistance.

The fabrication techniques of Al MMCs play a major role in the improvement of mechanical and tribological properties. Many techniques were developed for producing particulate reinforced Al MMCs, such as powder metallurgy [9], friction stir processing [10], stir casting and squeeze casting [11]. Based on expertise and through literature representation of the above methods, stir casting technique was supposed to be the simplest and the most economical process for fabricating

Corresponding author: K. SOORYA PRAKASH; Tel:+91-9443654639; E-mail: k_soorya@yahoo.co.in
DOI: 10.1016/S1003-6326(15)64036-5

particulate reinforced MMCs [12]. Uniform distribution of reinforcement is obtained by pre-heating it in graphite crucible maintained under an inert atmosphere with two-step stirring action until the matrix alloy is completely melted. Aluminum-based silicon carbide particulate metal matrix composites fabricated using this technique showed an increasing trend in hardness and impact strength values with the increase in volume fraction of SiC [13]. Experiments prove that the stir casting specimens have higher mechanical strength than the powder metallurgy specimen [14].

The tribological properties such as wear rate and coefficient of friction are considered to be the major factors controlling the performance of any MMC. In general, friction and wear behaviors of Al MMCs are generated from pin-on-disc tests. In all those tests, pins of Al MMCs slide against EN32 hardened steel disc or cast iron disc [15]. The results revealed that as the SiC content increases, the wear rate decreases, but for coefficient of friction, reverse trend can be observed [16]. It is well within the discussion of researchers that the applied load and sliding velocity affect the wear rate of composite materials wherein the wear rate increases with the increase in sliding speed and load [8,17]. At high sliding velocities, composites with higher content reinforcement exhibit higher wear resistance [18]. The addition of reinforcement to aluminum matrix alloys affects the transition from mild wear to severe wear, and thereby increases the wear resistance of composite materials [19−22], but the effect may be adverse depending on the matrix hardness [23] and on the wear mechanism of composite materials [24]. Therefore, it is indispensable to consider the factors such as mass fraction of reinforcement, size, load, sliding velocity and distance while determining the wear behavior of a material.

The application of design of experiment (DOE) concepts like Taguchi and response surface methodology has gained significance in recent years as these are supportive in providing the hierarchical rank order of the information on the influence of various parameters and their combined effects. The influence of parameters like sliding speed, sliding distance, normal load, and mass fraction of reinforcements on tribological behavior can be analyzed by utilizing an orthogonal array and analysis of variance (ANOVA) technique [25]. The widely used method for predicting response variables is regression analysis as it can predict the variables with minimal error [26].

In the present study, an attempt was made to understand and expose the influence of wear parameters such as sliding velocity, applied load, sliding distance, reinforcement size and mass fraction of reinforcement on the dry sliding wear behavior of the novel Al 6061/rock dust composite using Taguch's DOE. The combined effect of these parameters and their interaction were investigated using ANOVA technique.

2 Experimental

2.1 Materials

Aluminium 6061 alloy was stir-cast with rock dust as reinforcement so as to fabricate Al 6061/rock dust composites. The chemical composition of Al 6061 alloy is shown in Table 1. Rock dust was collected from quarries and Table 2 presents the detail of its chemical composition. The temperature of the furnace was precisely measured and accurately controlled (±1ºC) using two thermocouples and a PID controller. The experimental setup used a 1HP motor to rotate the stirrer at different speeds; a hydraulic lifting mechanism was used to bring the stirrer in contact with composite material.

Table 1 Chemical composition of Al 6061 alloy (mass fraction, %)

Mg	Si	Fe	Cu	Ti	Cr	Zn	Mn	Al
0.88	0.65	0.24	0.23	0.1	0.14	0.08	0.03	Bal.

Table 2 Chemical composition of rock dust (mass fraction, %)

SiO_2	Al_2O_3	Fe_2O_3	CaO	MgO
51	18.4	9.29	10.2	5.0

Na_2O	K_2O	TiO_2	Others
2.1	0.59	0.78	Bal.

Simultaneously, a measured quantity of rock dust weighed using digital electronic weighing machine was kept in a preheating furnace and preheated up to 600 °C. The preheated rock dust particles were added to the molten metal. The mixture was then kept in a furnace and heated to about 720 °C. The melt was subsequently stirred at 900 r/min using a stirrer attached to the variable speed motor. The furnace temperature was kept constant at 720 °C for 10 min; magnesium with mass fraction of 1.5% was added to increase the wettability. Then, the molten metal was poured into the mould and the required composite was obtained. The same procedure was repeated for fabricating all other compositions as tabulated in Table 3.

The cast Al 6061/rockdust composites were machined to the required specimen size for conducting various tests. SEM images of the novel composites under the specified compositions as given in Table 3 are acquired and shown in Fig. 1. From SEM images, it is evident that the reinforcement is properly mixed with the matrix material and also clearly exhibits the presence of Si particles due to rock dust reinforcements.

Table 3 Parameters of composite specimens

Sample No.	Reinforcement size/μm	Mass fraction of reinforcement/%	Density/ (g·cm^{-3})
1	10	5	2.710
2	10	10	2.694
3	10	15	2.751
4	20	5	2.732
5	20	10	2.781
6	20	15	2.733
7	30	5	2.804
8	30	10	2.666
9	30	15	2.694

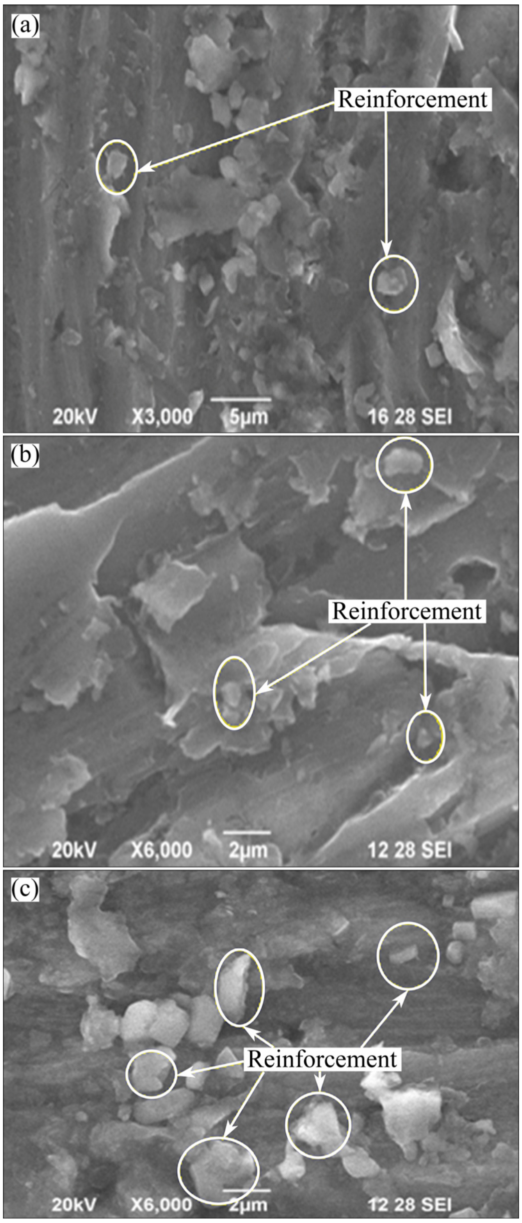

Fig. 1 SEM images of different composites: (a) 10 μm, 5% reinforcement; (b) 20 μm, 10% reinforcement; (c) 30 μm, 15% reinforcement

Reinforcement size, mass fraction of reinforcement and their corresponding density values for each composite sample are given in Table 3. Also from Table 3, it is evident that the density of the developed composite is higher than that of the unreinforced aluminium alloy which approximately equals 2.7g/cm^3. Brinell hardness value (BHN) of the composite increases with the increase in reinforcement size and its mass fraction; therefore, the outcome of this study correlates with early researches that material hardness has greater influence on wear resistance [27]. The same is clearly depicted in Fig. 2.

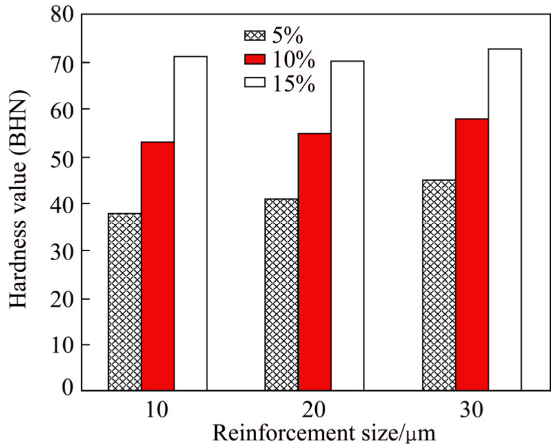

Fig. 2 Hardness value of MMC with corresponding reinforcement size and its mass fraction

2.2 Wear test

Pin-on-disc method was used to evaluate the specific wear rate of the specimen's sliding surfaces. The tests were conducted under dry laboratory conditions according to ASTM G99−95 standards. Schematic view of the pin-on-disc setup is shown in Fig. 3. The tests were carried out by applying normal loads of 10, 20, and 30 N and different sliding distances of 1, 2 and 3 km at three different sliding velocities of 2, 3 and 4 m/s, respectively. The disc material was made of EN32 steel with a hardness of HRC 65. The MMC samples were

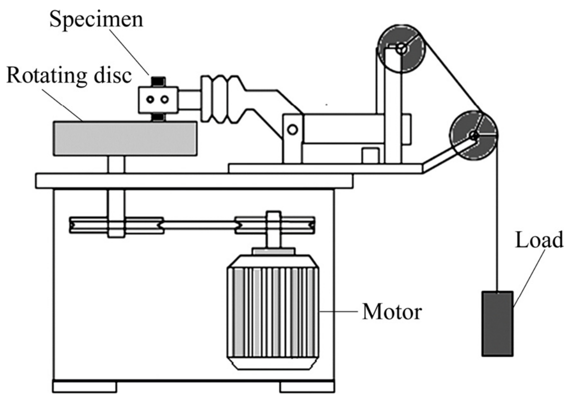

Fig. 3 Schematic representation of pin-on-disc setup

prepared as pins with regular dimensions of 8 mm × 8 mm with 40 mm in height. The pins slide on the disk at a track radius of 100 mm, the end surfaces of test sample are flat and polished with metallographic alloy before testing. Conventional aluminum alloy polishing technique was adhered to make the contact surfaces of the composite specimen on hand ready for wear test. In order to obtain more precise values of the wear rate, each trial was performed twice for the end surfaces prepared. At the end of each test, the pin was weighed and the differences between the initial and final masses were taken as a measure of slide mass loss. The average value of the wear rate was then used for further calculations so as to reduce the error. The specific wear rate (W) was calculated using the following equation:

$$W = \frac{\Delta m}{\rho t v_\mathrm{s} F_\mathrm{n}} \tag{1}$$

where Δm is the mass loss on the pin samples (g), ρ is the density of the test sample (g/mm^3), t is the test duration (s), v_s is the sliding velocity (m/s), F_n is the applied load (N) and W is the wear rate (mm^3/m).

2.3 Experimental design

The experiments were carried out to analyze the influence of testing parameters on wear rate of the composite material based on Taguchi method wherein the experimental results are transformed into a signal-to-noise (S/N) ratio for analysis. The test parameters, their codes and levels are given in Table 4. Taguchi's the-smaller-the-better performance characteristic was considered since the performance was measured in terms of wear rate, generally expected to be as low as possible. Moreover, analysis of variance (ANOVA) was performed to determine the statistically significant parameters.

Table 4 Control factors and their levels

Code	Control factor	Level 1	Level 2	Level 3
A	Reinforcement particle size/μm	10	20	30
B	Mass fraction of reinforcement/%	5	10	15
C	Applied load/N	10	20	30
D	Sliding velocity/(m·s^{-1})	2	3	4
E	Sliding distance/km	1	2	3

A standard Taguchi experimental plan with L27 (3^3) orthogonal array was chosen for the statistical analysis. The experimental results of wear rate are further transformed into a signal-to-noise ratio which is evaluated as the logarithmic transformation of loss function and the expression is as follows:

$$\frac{S}{N} = -10\lg\left(\frac{1}{n}\sum Y_i^2\right) \tag{2}$$

where n is the number of observations, Y_i is the measured value of wear rate. It is suggested that quality characteristics are optimized when the S/N response is as small as possible.

3 Results and discussion

3.1 Analysis of control factors

The influence of each control factor (A, B, C, D and E) on the wear rate was determined with S/N response table using Minitab 16.1 software. Table 5 shows the orthogonal array and experimental results for wear rates with calculated S/N ratio. The S/N response table for wear rate presented in Table 6 illustrates the calculated S/N ratio for each level of control factors. The control factor that has the strongest influence is determined depending on the δ value shown in Table 6. δ equals the difference between maximum and minimum S/N ratio for a particular control factor. It is obvious that higher δ value denotes greater influence of the corresponding control factor.

It is clear from Table 6 that the strongest influence is exerted by applied load, followed by other considered significant parameters viz reinforcement size, mass fraction of reinforcement, sliding velocity and sliding distance, respectively.

Taguchi's technique analyzes S/N ratio using a conceptual approach by graphing the special effects and visually make out the significance of various other influencing factors. The influence of each control factor on wear rate is graphically represented by Figs. 4 and 5, which help to easily determine the optimum levels for each control factor. With "mean of means", it is referred as to firstly take the mean of individual values within the team (team consists of two wear rate values observed through individual trials) and then the mean of team means within the group comprising of 27 trials was calculated.

Response graphs show the variation of S/N ratio with the change in control factors from one level to the other level. Figure 4 suggests the optimum condition for the minimum wear rate in combination of $A_1B_1C_3D_1E_3$ levels of control factors. In order to reduce wear rate, factors such as mass fraction of reinforcement and sliding velocity should be lowered while reducing the reinforcement size. Again, it is proven that applied load has the most dominating effect on wear rate of the composite. Researchers have reported that wear rate of the composite was superior to the matrix alloy at all loads [23]. Because of small magnitude of loads considered, the wear rate decreases as load increases. At

Table 5 Orthogonal array and results for Al 6061/rock dust composites

Experiment No.	Reinforcement size/μm	Mass fraction of reinforcement/%	Applied load/N	Sliding velocity/($m \cdot s^{-1}$)	Sliding distance/km	Average wear rate/(10^{-3} $mm^3 \cdot m^{-1}$)	S/N ratio
1	10	5	10	2	1	0.607	64.33623
2	10	5	10	2	2	0.584	64.67174
3	10	5	10	2	3	0.575	64.80664
4	10	10	20	3	1	0.498	66.05541
5	10	10	20	3	2	0.478	66.41144
6	10	10	20	3	3	0.458	66.78269
7	10	15	30	4	1	0.681	63.33706
8	10	15	30	4	2	0.584	64.67174
9	10	15	30	4	3	0.588	64.61245
10	20	5	20	4	1	0.589	64.59769
11	20	5	20	4	2	0.672	63.45261
12	20	5	20	4	3	0.653	63.70174
13	20	10	30	2	1	0.557	65.08290
14	20	10	30	2	2	0.494	66.12546
15	20	10	30	2	3	0.471	66.53958
16	20	15	10	3	1	1.307	57.67449
17	20	15	10	3	2	1.108	59.10920
18	20	15	10	3	3	0.992	60.06977
19	30	5	30	3	1	0.592	64.55357
20	30	5	30	3	2	0.572	64.85208
21	30	5	30	3	3	0.533	65.46546
22	30	10	10	4	1	1.359	57.33561
23	30	10	10	4	2	1.248	58.07571
24	30	10	10	4	3	1.289	57.79494
25	30	15	20	2	1	1.099	59.18005
26	30	15	20	2	2	0.842	61.49376
27	30	15	20	2	3	0.812	61.80888

Table 6 Response to S/N ratio for wear rate (smaller S/N ratio is better)

Level	Reinforcement size	Mass fraction of reinforcement	Applied load	Sliding velocity	Sliding distance
1	65.08	64.49	60.43	63.78	62.46
2	62.93	63.36	63.72	63.44	63.21
3	61.17	61.33	65.03	61.95	63.51
δ	3.90	3.16	4.60	1.83	1.05
Rank	2	3	1	4	5

an applied load of 10 N, wear loss is high and gets decreased while increasing load to 20 N, as shown in Fig. 4. Even though the wear loss decreases with further increase in load from 20 to 30 N, the wear rate is higher compared with the former (10−20 N). Further increase in load will possibly result only in increased wear rate. Hence, the current study also acknowledges that the wear behavior of the composite based on pure aluminum matrix with various reinforcements increases with the increase in the applied load [28,29].

Reinforcement size is the second most effective factor on the wear rate of the composite. It is observed that the wear rate of the composite increases with the increase in reinforcement size and vice versa. Smaller size reinforcements fill the pores in the matrix materials, hence increases the bonding strength and concurrent

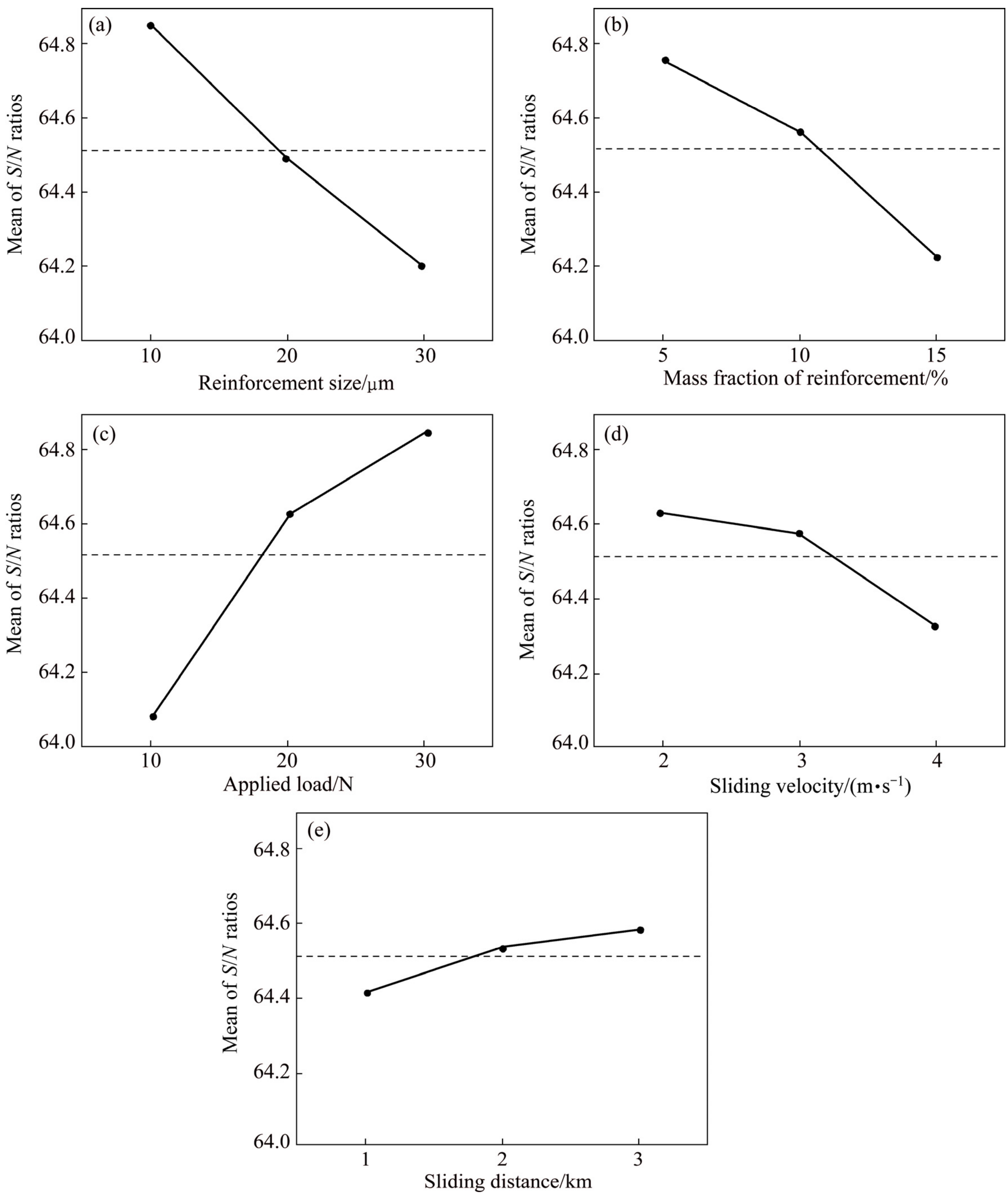

Fig. 4 Effect of various parameters on *S*/*N* ratio for wear rate (smaller *S*/*N* ratio is better)

hardness which results in higher wear resistance.

The third factor influencing the wear rate of the composite is the mass fraction of reinforcement. Upon clear notification, it is concluded that the wear rate of the composite increases with the increase of rock dust content in the composite. This occurrence reveals that higher content of reinforcements decreases the bonding strength. Figure 6 shows the EDAX pattern of the composite with 10 μm and 5% reinforcement. It is seen from the peak that the silica present in the rock dust has been mixed evenly within the composite. Hence, it is further proved that the addition of rock dust improves the wear resistance. The result has a good coherence with earlier researches of which the presence of ceramic reinforcements increases the wear resistance of aluminum matrix alloys at low loads [19], but the wear resistance is less at higher loads.

The fourth influencing factor of the developed composite is the sliding velocity. From the observance over the experimental data, it is noticeable that the wear rate of the composite increases with the increase in sliding velocity. The friction and wear properties of the

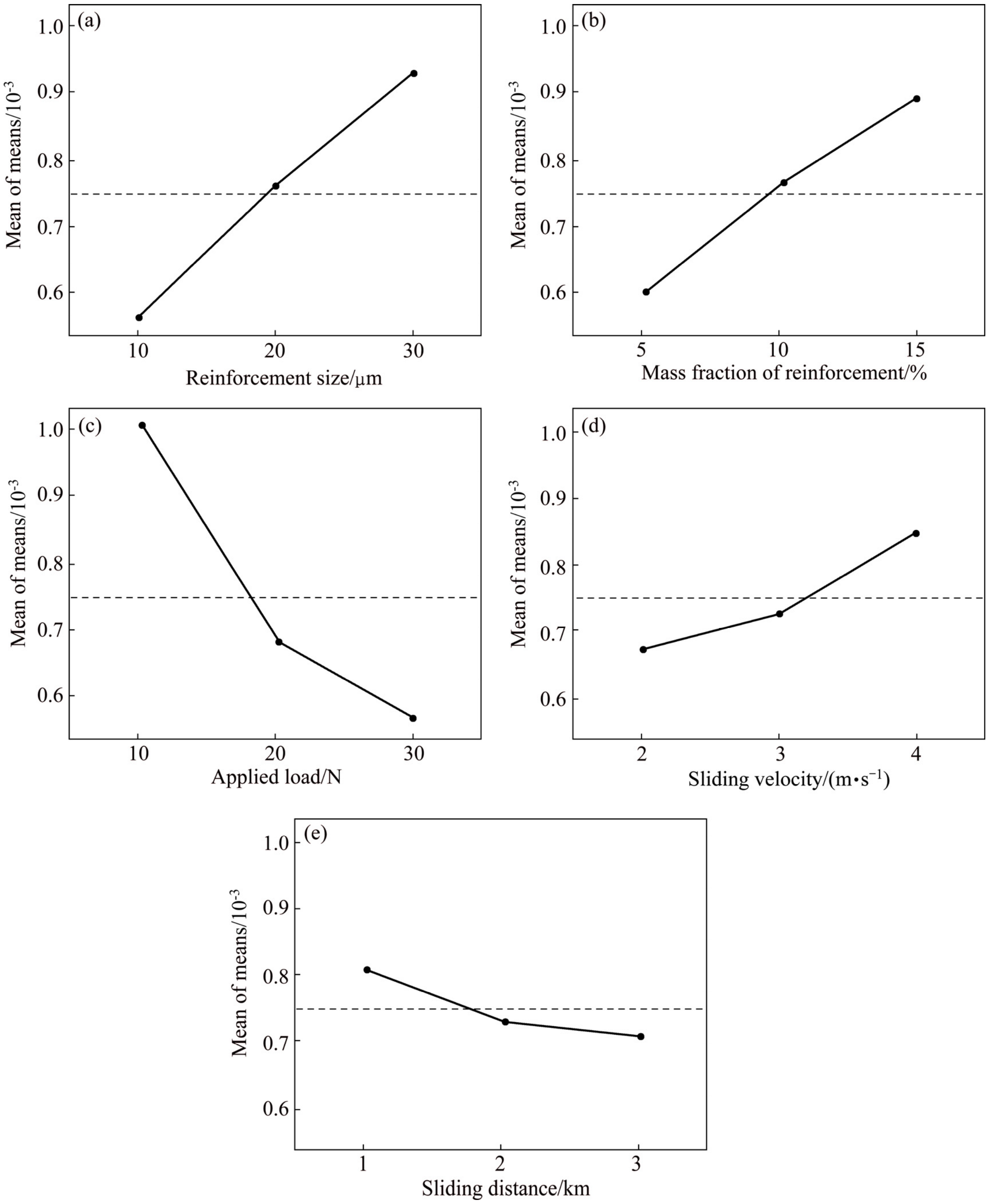

Fig. 5 Effect of various parameters on mean of means for wear rate

reinforced composites were studied [30−32] and the results of similar other researches also show that wear rate of materials increases with sufficient increment in sliding velocity.

The least influencing factor for the wear rate is sliding distance, when compared with all other factors. With the increase in sliding distance from 1 to 2 km, the volume loss of the composite decreases initially, and for further increase in distance from 2 to 3 km, the wear rate of the composite is higher compared with that of the former. This behaviour depicts that further increase in sliding distance will increase the wear rate of the composite. As the sliding distance increases, the increase in surface temperature is unavoidable, resulting in softening of material and high wear loss [33].

3.2 ANOVA

The ANOVA was used to investigate which of the design parameter significantly affects the quality characteristics of the composite. It was performed by separating the total variability of the *S*/*N* ratios into contributions by each of the design parameters and the errors.

The total variability of *S*/*N* ratio was measured by

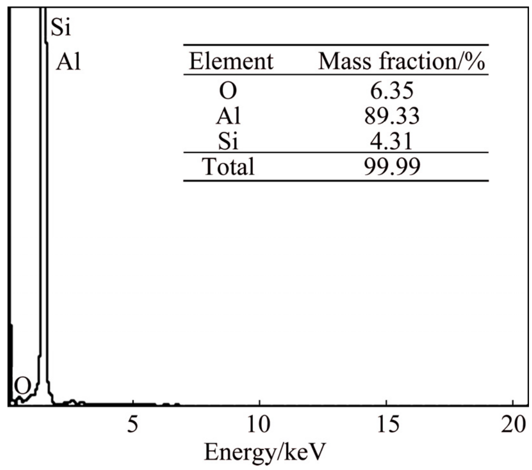

Fig. 6 EDAX pattern of composite with 5% reinforcement of 10 μm in size

the sum of the squared deviations from the total mean *S*/*N* ratio. The calculated Fisher's value (*F*) shows that factor *C* has very great influence and factor *E* has small influence on the wear rate of the composite (Table 7). Generally, if F>4, the relative design parameter has a significant effect on the quality characteristic of the composite. Thus, *F* value indicates that there is a significant effect on all the factors of composite. The last column of Table 7 indicates the percentage of contribution (P_r) of each factor on the wear rate of the composite. It shows that the applied load, reinforcement size, mass fraction of reinforcement, sliding velocity and sliding distance have percentage of contribution (P_r) of 47.61%, 28.57%, 19.04%, 9.52% and 4.76%, respectively. From this, it is evident that the addition of rock dust influences wear performance of the material significantly and it can be further investigated by adding smaller size rock dust particles.

3.3 Regression model

The correlation between the control factors (reinforcement size (*A*), mass fraction of reinforcement (*B*), applied load (*C*), sliding velocity (*D*) and sliding distance (*E*)) and the wear rate (*W*) was obtained by multiple linear regression technique and represented as follows:

$$W= 3.67\times10^{-4} +1.8\times10^{-5}A+2.9\times10^{-5}B-2.2\times10^{-5}C+9.0\times10^{-5}D-5.0\times10^{-8}E \quad (3)$$

The correlation coefficient is R^2=0.929. The developed equation should be validated by confirmation test wherein the predicted results are compared with experimental values.

3.4 Confirmation test

The final step in design process is confirmation test. In this work, dry sliding wear test was conducted with a combination of levels and parameters to validate the statistical analysis. The preferred combination of the levels of the factors is indicated to be significant by the analytical methods and also to validate the conclusions drawn during the analysis phase. Table 8 shows the test parameters for conducting the dry sliding wear test. The reinforcement size and mass fraction of reinforcement were maintained constant (10 μm, 5%; 20 μm, 10%) for both experiments. Confirmation experiment was carried out and then the comparison between experimental values and computed values shows an error associated with dry sliding wear of composites varying from 3.10% to 6.59%.

3.5 SEM observations

The morphological changes on the worn out surface of Al 6061/rock dust composite developed are clearly visualized through SEM images summarized in Fig. 7.

Table 7 Analysis of variance for wear rate of composite

Source	DF	Seq SS/10^{-5}	Adj SS/10^{-5}	Adj MS/10^{-5}	F	P	P_r/%
Reinforcement size	2	0.06	0.06	0.03	66.76	0.000	28.57
Mass fraction of reinforcement	2	0.04	0.04	0.02	42.87	0.000	19.04
Applied load	2	0.10	0.10	0.05	105.80	0.000	47.61
Sliding velocity	2	0.02	0.02	0.01	16.96	0.000	9.52
Sliding distance	2	0.01	0.01	0.00	5.68	0.014	4.76
Error	16	0.01	0.01				
Total	26	0.22					

Table 8 Confirmation test parameters

Experiment No.	Load/N	Sliding velocity/ ($m\cdot s^{-1}$)	Sliding distance/km	Experimental wear rate/(10^{-3} $mm^3\cdot m^{-1}$)	Regression model wear rate/(10^{-3} $mm^3\cdot m^{-1}$)	Error/%
1	12	2.5	1.2	0.612	0.593	3.10
2	24	3.5	2.2	0.743	0.694	6.59

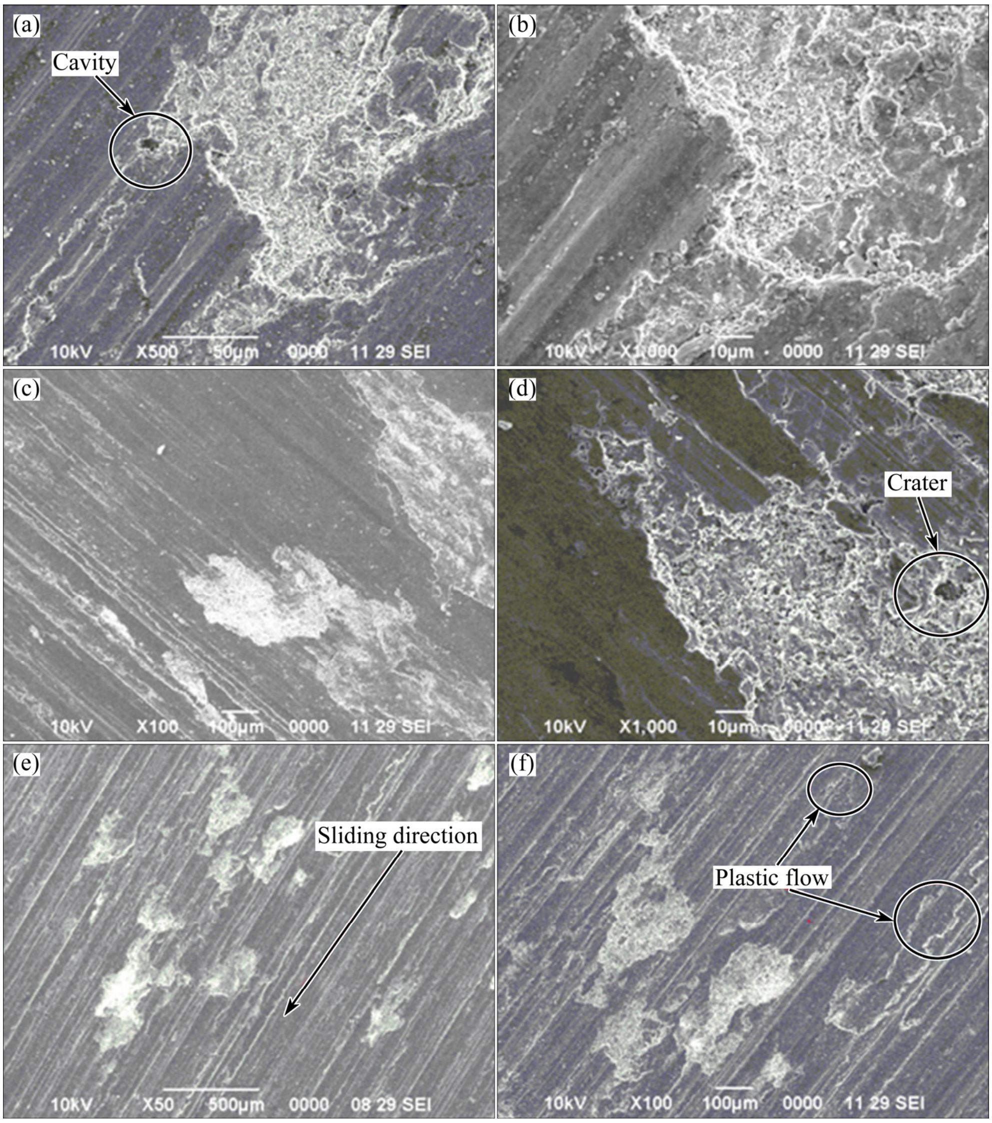

Fig. 7 SEM images of worn surfaces of Al 6061/rock dust composites with different reinforcement sizes and contents: (a) 10 μm, 5%; (b) 10 μm, 10%; (c) 20 μm, 10%; (d) 20 μm, 15%; (e) 30 μm, 10%; (f) 30 μm, 15%

In a naked view, it could be well furnished that wear rate of rock dust reinforced Al 6061 alloy is less when compared with that of unreinforced alloy.

In Fig. 7(a), the micrograph of Al 6061/10 μm/5% of reinforcement at a load of 10 N with sliding velocity of 2 m/s for a sliding distance of 1 km is shown, and upon keen observation it is obvious to highlight that less area of craters is a sign of minimum wear in these areas. Figure 7(b) shows the SEM image of Al 6061/10 μm/ 10% of reinforcement at load of 30 N with sliding velocity of 3 m/s for a sliding distance of 3 km. It is observed that the plastic flow occurs on the surface due to the increase in velocity and the sliding distance. Observance over Fig. 7(d), Al6061/20 μm/15% of reinforcement at load of 20 N with sliding velocity of 3 m/s for a sliding distance of 3 km shows large cavities in the subsurface layer, indicating severe loss of material. The reason for these larger cavities is that when the material slides over other material at higher velocities, the temperature on sliding surface increases and softens the parent material which results in particle pull-out. The overall picture of the SEM images points up as the mass fraction of the reinforcement decreases these ridges and grooves become shallower and plastic flow zone of the material decreases. The above artifact could be regarded as a superior level of indication confirming greater resistance to wear. Hence, as the research on the current material correlates well with the property values of other comparable rival materials, it is an inevitable fact that the developed composite could also be affiliated to the existing stream of composites developed on the similar platform. From now, this novel material can be well utilized in manufacture of automobile accessories like brake components and for various products of such other similar applications.

4 Conclusions

1) Taguchi's technique is used to find the optimum conditions of dry sliding wear of Al 6061/rock dust composite.

2) The wear rate is dominated by different parameters in the order of applied load, reinforcement size, mass fraction of reinforcement, sliding velocity and sliding distance. The optimum condition for minimum wear rate falls in the combination of $A_1B_1C_3D_1E_3$ levels of control factors. The ANOVA test concludes that as the reinforcement size and the mass fraction of reinforcement decrease, the wear rate decreases. The applied load (47.61% of contribution) has the highest statistical influence on the wear rate of the composite among all other factors viz reinforcement size (28.57% of contribution), mass fraction of reinforcement (19.04% of contribution), sliding velocity (9.52% of contribution) and sliding distance (4.76% of contribution). Abrasive wear observed in the SEM micrograph reveals that as the reinforcement size and mass fraction of reinforcement decrease, the ridges and grooves become shallow, indicating a resistant behavior to wear.

3) Confirmation experiment was carried out and a comparison was made between experimental values and computed values, showing an error associated with dry sliding wear of composites varying from 3.10% to 6.59%.

4) Wet sliding wear behavior of the novel composite can be predicted with various parameters by choosing proper lubricant and then high temperature wear can also be tested both experimentally and mathematically.

References

[1] TJONG S C, MA Z Y. Micro structural and mechanical characteristics of in situ metal matrix composites [J]. Materials Science and Engineering R, 2000, 29: 49−113.

[2] TU J P, RONG W, GUO S Y, YANG Y Z. Dry sliding wear behavior of in situ Cu−TiB_2 nano composites against medium carbon steel [J]. Wear, 2003, 255: 832−835.

[3] SANNINO A P, RACK H J. Dry sliding wear of discontinuously reinforced aluminum composites: Review and discussion [J]. Wear, 1995, 189: 1−19.

[4] MIRACLE D B. Metal matrix composites-from science to technological significance [J]. Composite Science Technology, 2005, 65: 2526−2540.

[5] SURAPPA M K, PRASAD S V, ROHATGI P K. Wear and abrasion of cast Al–alumina particle composites [J]. Wear, 1982, 77: 295−302.

[6] PRAMILABAI B N, RAMASHESH B S, SURAPPA M K. Dry sliding wear of A356−Al−SiC_P composites [J]. Wear, 1992, 157: 295−304.

[7] MAHENDRA K V, RADHAKRISHNA K. Characterization of stir cast Al−Cu−(fly ash/SiC) hybrid metal matrix composites [J]. Journal of Composite Materials, 2010, 44(8): 989−1005.

[8] BASAVARAJAPPA S, CHANDRAMOHAN G, MUKUND K, ASHWIN M, PRABU M. Dry sliding wear behaviour of Al2219/SiC_p−Gr hybrid metal matrix composites [J]. Journal of Material Engineering Performance, 2006, 15: 668−674.

[9] HAN N L, WANG Z G, SUN L Z. Low cycle fatigue behaviour of SiC_p reinforced aluminium matrix composite at ambient and elevated temperature [J]. Scripta Metallurgica et Materialia, 1995, 32: 1739−1745.

[10] DEVARAJU A, KUMAR A, KOTIVEERACHARI B. Influence of addition of Gr_p/Al_2O_{3p} with SiC_p on wear properties of aluminum alloy 6061−T6 hybrid composites via friction stir processing [J]. Transactions of Nonferrous Metals Society of China, 2013, 23(5): 1275−1280.

[11] HWU B K, LIN S J, JAHN M T. The interfacial compounds and SEM fractography of squeeze-cast SiC_p/6061 Al composites [J]. Material Science and Engineering A, 1996, 206: 110−119.

[12] HASHIM J, LOONEY L, HASHMI M S J. Metal matrix composites: production by the stir casting method [J]. Journal of Material Processing Technology, 1999, 92−93: 1−7.

[13] MANOJ S, DEEPAK DWIVEDI D, LAKHVIR S, VIKAS C. Development of aluminium based silicon carbide particulate metal matrix composite [J]. Journal of Minerals and Materials Characterization and Engineering, 2009, 8: 455−467.

[14] JAYASEELAN V, KALAICHELVAN K, KANNAN M, VIJAY ANANTH S. Extrusion characterizes of Al/SiC by different manufacturing process [J]. International Journal of Applied Engineering Research, 2010, 1: 194−199.

[15] ZHU H G, AI Y L, MIN J, WU Q, WANG H Z. Dry sliding wear behavior of Al-based composites fabricated by exothermic dispersion reaction in an Al−ZrO_2−C system [J]. Wear, 2010, 268: 1465−1471.

[16] RAO R N, DAS S. Effect of SiC content and sliding speed on the wear behaviour of aluminium matrix composites [J]. Materials and Design, 2011, 32: 1066−1071.

[17] KWOK J K M, LIM S C. High-speed tribological properties of some Al/SiC_p composites. I: Frictional and wear-rate characteristics [J]. Composite Science and Technology, 1999, 59: 55−63.

[18] MA Z Y, LIANG Y N, ZHANG Y Z, LU Y X, BI J. Sliding wear behaviour of SiC particle reinforced 2024 Al alloy composites [J]. Materials Science and Technology, 1996, 12: 751−756.

[19] ALPAS A T, ZHANG J. Effect of microstructure (particulate size and volume fraction) and counter face material on the sliding wear resistance of particulate-reinforced aluminum matrix composites [J]. Metallurgical and Materials Transactions A, 1994, 25: 969−983.

[20] BASAVARAJAPPA S, CHANDRAMOHAN G, SUBRAMANIAN R, CHANDRASEKAR A. Dry sliding wear behaviour of Al 2219/SiC metal matrix composites [J]. Materials Science—Poland, 2006, 24: 357−66.

[21] DEBDAS R, BIKRAMJIT B, AMITAVA B M. Tribological properties of Ti-aluminide reinforced Al-based in situ metal matrix composites [J]. Intermetallics, 2005, 13: 733−740.

[22] VENKATARAMAN B, SUNDARARAJAN G. The sliding wear behaviour of Al−SiC particulate composites. I: Macrobehaviour [J]. Acta Materialia, 1996, 44: 451−460.

[23] RANJIT B, SURAPPA M K. Sliding wear behavior of Al−Li−SiC_p composites [J]. Wear, 2008, 265: 1756−1766.

[24] RODRIGUEZ J, POZA P, GARRIDO MA, RICO A. Dry sliding wear behaviour of aluminium–lithium alloys reinforced with SiC particles [J]. Wear, 2007, 262: 292−300.

[25] BASAVARAJAPPA S, CHANDRAMOHAN G. Wear studies on metal matrix composites: A Taguchi approach [J]. Journal of Material Science and Technology, 2005, 21: 845−850.

[26] SUBRAMANIAN M, SAKTHIVEL M, SOORYAPRAKASH K, SUDHAKARAN R. Optimization of end mill tool geometry parameters for Al7075-T6 machining operations based on vibration amplitude by response surface methodology [J]. Measurement, 2013,

46: 4005−4022.
[27] MAZAHERY A, SHABANI M O. Microstructural and abrasive wear properties of SiC reinforced aluminum-based composite produced by compocasting [J]. Transactions of Nonferrous Metals Society of China, 2013, 23(7): 1905−1914.
[28] ZHANG L, HE X B, QU X H, DUAN B H, LU X, QIN M L. Dry sliding wear properties of high volume fraction SiC_p/Cu composites produced by pressure less infiltration [J]. Wear, 2008, 265: 1848−1856.
[29] MANISH R, VENKATARAMAN B, BHANUPRASAD V V, MAHAJAN Y R, SUNDARARAJAN G. The effects of particulate reinforcement on the sliding wear behavior of aluminium–matrix composites [J]. Metallurgical Transactions A, 1992, 23: 2833−2847.
[30] LIU L, LI W W, TANG Y P, SHEN B, HU W B. Friction and wear properties of short carbon fiber reinforced aluminum matrix composites [J]. Wear, 2009, 266: 733−738.
[31] NATARAJAN N, VIJAYARANGAN S, RAJENDRAN I. Wear behaviour of A356/25SiC_p aluminium matrix composites sliding against automobile friction material [J]. Wear, 2006, 261: 812−822.
[32] SATO A, MEHRABIAN R. Aluminum matrix composites: Fabrication and properties [J]. Metallurgical Transactions B, 1976, 7: 443−451.
[33] PAULO DAVIM J. Tribology of composite materials [M]. New York: NOVA Science Publishers, 2010.

6061 铝合金/岩粉复合材料的干滑动磨损行为

K. SOORYA PRAKASH[1], A. KANAGARAJ[2], P. M. GOPAL[1]

1. Department of Mechanical Engineering, Anna University Regional Campus, Coimbatore 641046, India;
2. Department of Mechanical Engineering, Akshaya College of Engineering and Technology, Coimbatore 642109, India

摘　要：研究岩粉尺寸(10~30 μm)和质量分数(5%~15%)对搅拌铸造法制备 6061 铝合金/岩粉复合材料密度、硬度和干滑动磨损行为的影响。在不同载荷、不同滑动速率和滑动距离条件下在销盘摩擦试验机上对复合材料进行干滑动摩擦磨损试验。采用 Taguchi 法进行正交试验(L27)设计，并对实验结果进行方差分析。结果表明，载荷和增强相(岩粉)尺寸是影响复合材料样品比摩损率的主要因素，其次为增强相的质量分数、滑动速率、滑动距离，且其影响程度分别为 47.61%、28.57%、19.04%、9.52%和 4.76%。对所得回归方程的预测精度进行实验论证，结果显示，此回归方程能用于复合材料的磨损率的预测且预测误差很小。复合材料磨损表面的 SEM 结果表明，以岩粉作为增强相能改善铝合金材料的耐磨性能。

关键词：铝基复合材料；岩粉；搅拌铸造；磨损；方差分析

(Edited by Wei-ping CHEN)